Using Electrospray Ionization Mass Spectrometry to Explore the Interactions Among Polythymine Oligonucleotides, Ethidium Bromide, and Mercury Ions

Cheng-Kang Chiang,[a] Yang-Wei Lin,[a] Cho-Chun Hu,[b] and Huan-Tsung Chang[a]

[a] Department of Chemistry, National Taiwan University, Taipei, Taiwan
[b] Department of Applied Science, National Taitung University, Taitung, Taiwan

We have used electrospray ionization mass spectrometry (ESI-MS) and fluorescence and circular dichroism (CD) spectroscopy to explore the binding of ethidium bromide (EthBr) to non-self-complementary polythymine (polyT) strands in the absence and presence of Hg^{2+} ions. In the gas phase, ESI-MS revealed that Hg^{2+} ions have greater affinity, through $T–Hg^{2+}–T$ coordination, toward polyT strands than do other metal ions. These findings are consistent with our fluorescence and CD results obtained in solution; they revealed that more $T_{33}–EthBr–Hg^{2+}$ complexes existed upon increasing the concentrations of Hg^{2+} ions (from 0 to 50 μM). Surprisingly, the ESI-MS data indicated that the Hg^{2+} concentration dependence of the interaction between T_{33} and EthBr is biphasic. Our ESI-MS data revealed that the $T_{33}–EthBr–Hg^{2+}$ complexes formed with various stoichiometries depending on their relative concentrations of the components and the length of the DNA strand. When the concentrations of $T_{33}/EthBr/Hg^{2+}$ were 5/5/2.5 μM and 5/10/7.5 μM, 1:1:1 and 1:1:2 $T_{33}–EthBr–Hg^{2+}$ complexes were predominantly formed, respectively. Thus, Hg^{2+}-induced DNA conformational changes clearly affect the interactions between DNA and EthBr. (J Am Soc Mass Spectrom 2009, xx, xxx) © 2009 American Society for Mass Spectrometry

Studies of the interactions between Hg^{2+} ions and DNA are interesting because they affect many different areas of the brain and their associated functions, resulting in symptoms such as vision problems, deafness, and loss of muscle coordination [1]. It has long been known that Hg^{2+} ions interact strongly with DNA strands through thymine (T)–Hg^{2+}–T coordination [2]; indeed, taking advantage of such complexation allows the detection of Hg^{2+} ions through Hg^{2+}-induced conformational changes of DNA [3–5]. Recently, we presented a simple and rapid fluorescence assay, using the double-stranded DNA binding dye TOTO-3 and the polythymine oligonucleotide T_{33}, for the highly selective and sensitive detection of Hg^{2+} in aqueous solution [6]. In the presence of Hg^{2+} ions, T_{33} changes its conformation from a random coil to a hairpin-like structure, leading to increased fluorescence. The formation of T–Hg^{2+}–T complexes has been confirmed indirectly using fluorescence polarization spectroscopy, capillary electrophoresis (CE), circular dichroism (CD) spectroscopy, and melting temperature measurements [3–6]. At this time, no direct evidence of such interactions exist.

Electrospray ionization mass spectrometry (ESI-MS) has been used to investigate the interactions of small analytes with various types of DNA structures, including G-quadruplexes [7–11] and DNA duplexes [12–16]. For example, ESI-MS has provided evidence for the existence of interactions between perylene diimides and G-quadruplex DNA [17], ethidium bromide (EthBr) and DNA duplexes [18], and metal ions and single-/double-stranded DNA [19–22]. ESI-MS allows the transfer of noncovalently bound complexes in solution to the gas phase without disruption of the complexes [23]. Thus, ESI-MS techniques are powerful for obtaining biomolecular structures and for determining the concentrations of all species of interest.

In this study, we used fluorescence and CD spectroscopy and ESI-MS to investigate the interactions between polyT strands and Hg^{2+} ions in the absence and presence of EthBr. EthBr has been used widely in CE-based analyses of DNA [24–26]. In addition, it has been established that EthBr interacts with DNA triplexes and G-quadruplexes [9]. In this study, we investigated the roles played by the concentrations of Hg^{2+} and EthBr, the length of DNA, and the DNA:Hg^{2+}:

Address reprint requests to Dr. H.-T. Chang, Department of Chemistry, National Taiwan University, 1, Section 4, Roosevelt Road, Taipei 106, Taiwan. E-mail: changht@ntu.edu.tw

EthBr molar ratio in determining the interactions among DNA, Hg^{2+}, and EthBr.

Experimental

Chemicals

Ammonium acetate (NH_4OAc), metal ions (all nitrate salts), and other reagents were purchased from Aldrich (Milwaukee, WI, USA). EthBr was obtained from Pharmacia Biotech (Uppsala, Sweden). PolyTs (T_7, T_{15}, T_{33}, and T_{50}) were purchased from Integrated DNA Technology (Coralville, IA, USA).

ESI-MS

A Bruker esquire HCT mass spectrometer (Bremen, Germany) was operated in the negative mode with a capillary voltage of 2.5 kV; the dry gas flow rate was controlled at 3.0 L/min; the nebulizer was controlled at 13.0 psi, and dry temperature was set to 250 °C. Full scan MS spectra were recorded in the m/z range 250–1500 with 50 acquisitions per spectrum. To obtain stable electrospray signals, 20% MeOH was added to each of the injected solutions before ESI-MS measurement. Aliquots (10 μL) of metal ion solutions (10–500 μM) were added separately to NH_4OAc solutions (5 mM, pH 7.0, 0.1 mL), each containing one of the polyT oligonucleotides (5 μM) and EthBr (0–20 μM). The mixtures were equilibrated at ambient temperature for 30 min. The DNA samples were infused directly at 3 μL/min into the mass spectrometer.

We calculated the fraction of T_{33}–Hg^{2+} complexes using eq 1 according to a reported method [17]

Fraction of T_{33}–Hg^{2+} complexes

$$= \frac{I_{(1:1)} + I_{(1:2)} + I_{(1:3)} + \dots + I_{(1:n)}}{I_{T_{33}} + I_{(1:1)} + I_{(1:2)} + I_{(1:3)} + \dots + I_{(1:n)}} \quad (1)$$

where I_{T33} and $I_{(1:n)}$ represent the intensity of T_{33} and T_{33}–$n Hg^{2+}$ complex, respectively, n is integral.

CD Spectroscopy

Samples (1.0 mL) containing T_{33} (1 μM), Hg^{2+} (0–5 μM), EthBr (0–5 μM), and NH_4OAc (5 mM, pH 7.0) in the presence of 20% MeOH were equilibrated at room temperature for 30 min before CD measurements. CD spectra of these mixtures were recorded in the wavelength range 240–320 nm using a J-815 CD spectropolarimeter (JASCO, Easton, MD, USA). A quartz cell (ChromTech GmbH, Idstein, Germany) having a path length of 1 cm was used as the sample vial to obtain the CD spectra, recorded from 240 to 320 nm at 0.1 nm intervals.

Fluorescence Spectroscopy

A Cary Eclipse fluorescence spectrophotometer (Varian, Palo Alto, CA, USA) was used to record the fluorescence spectra of mixtures similar to those used for the CD spectroscopy measurements. The fluorescence intensities of mixtures containing T_{33} (1 μM) and EthBr (1 μM) in the absence and presence of Hg^{2+} (0–50 μM) at 610 nm were recorded when excited at 530 nm. The Job method of continuous variation was used to determine the stoichiometries of the T_{33}–EthBr–Hg^{2+} complexes in the presence of Hg^{2+} (0–50 μM). To determine the stoichiometries of the complexes, the molar fraction of EthBr (X_{EthBr}) was varied, while the total concentration of EthBr and T_{33} was maintained at 1 μM.

Results and Discussion

ESI-MS of T_{33}

Figure 1a displays the mass spectrum of a solution of T_{33} (5 μM) in the presence of 20% MeOH. We assign the signals at m/z 906.0, 830.4, 766.4, 711.6, 664.1, and 622.5 to the ions $[T_{33} - 11H^+]^{11-}$, $[T_{33} - 12H^+]^{12-}$, $[T_{33} - 13H^+]^{13-}$, $[T_{33} - 14H^+]^{14-}$, $[T_{33} - 15H^+]^{15-}$, and $[T_{33} - 16H^+]^{16-}$, respectively. The broadness of most of these peaks results mainly from the counterion condensation of T_{33} during droplet evaporation and the formation of Na^+ and/or K^+ adducts of T_{33} [7, 27]. Upon increasing the NH_4OAc concentration to 5 mM (Figure 1b), the most abundant signals were those of the $[T_{33} - 13H^+]^{13-}$, with good mass spectra sensitivity. The interfering peaks at m/z 556.1, 680.6, and 980.0 are assigned to the $[7NH_4OAc + H_2O - H^+]^-$, $[17NH_4OAc + 3H_2O - 2H^+]^{2-}$, and $[25NH_4OAc + 2H_2O - 2H^+]^{2-}$, respectively. Upon further increasing NH_4OAc concentration (Figure 1c; 50 mM NH_4OAc), the analyte ionization was suppressed. Thus, the optimal concentration of NH_4OAc was chosen at 5 mM for further ESI-MS measurements.

Interactions Between T_{33} and Metal Ions

Figure 2a displays the ESI-MS spectrum of T_{33} (5.0 μM) recorded in the presence of 1 μM Hg^{2+} ions; we assign the peak appearing at m/z 781.7 to the $[T_{33} + Hg^{2+} - 15H^+]^{13-}$ ion. Upon increasing the concentration of Hg^{2+}, the intensity of this peak increased. For example, Using eq 1, we calculated the fraction of the intensity of the signal for the $[T_{33} + Hg^{2+} - 15H^+]^{13-}$ ion to the total intensity of the signals for T_{33} species (i.e., $[T_{33} - 13H^+]^{13-} + [T_{33} + Hg^{2+} - 15H^+]^{13-}$). The fraction increased from 11% to 20% upon increasing the concentration of Hg^{2+} from 1.0 to 5.0 μM (Figure 2b). Figure 2c reveals that increasing the concentration of Hg^{2+} ions to 10.0 μM caused the fractional intensity of the signal for the $[T_{33} + Hg^{2+} - 15H^+]^{13-}$ ions to increase to 23%. In addition, a peak representing the $[T_{33} + 2 Hg^{2+} - 17H^+]^{13-}$ ion appeared (fractional intensity: 8%). At
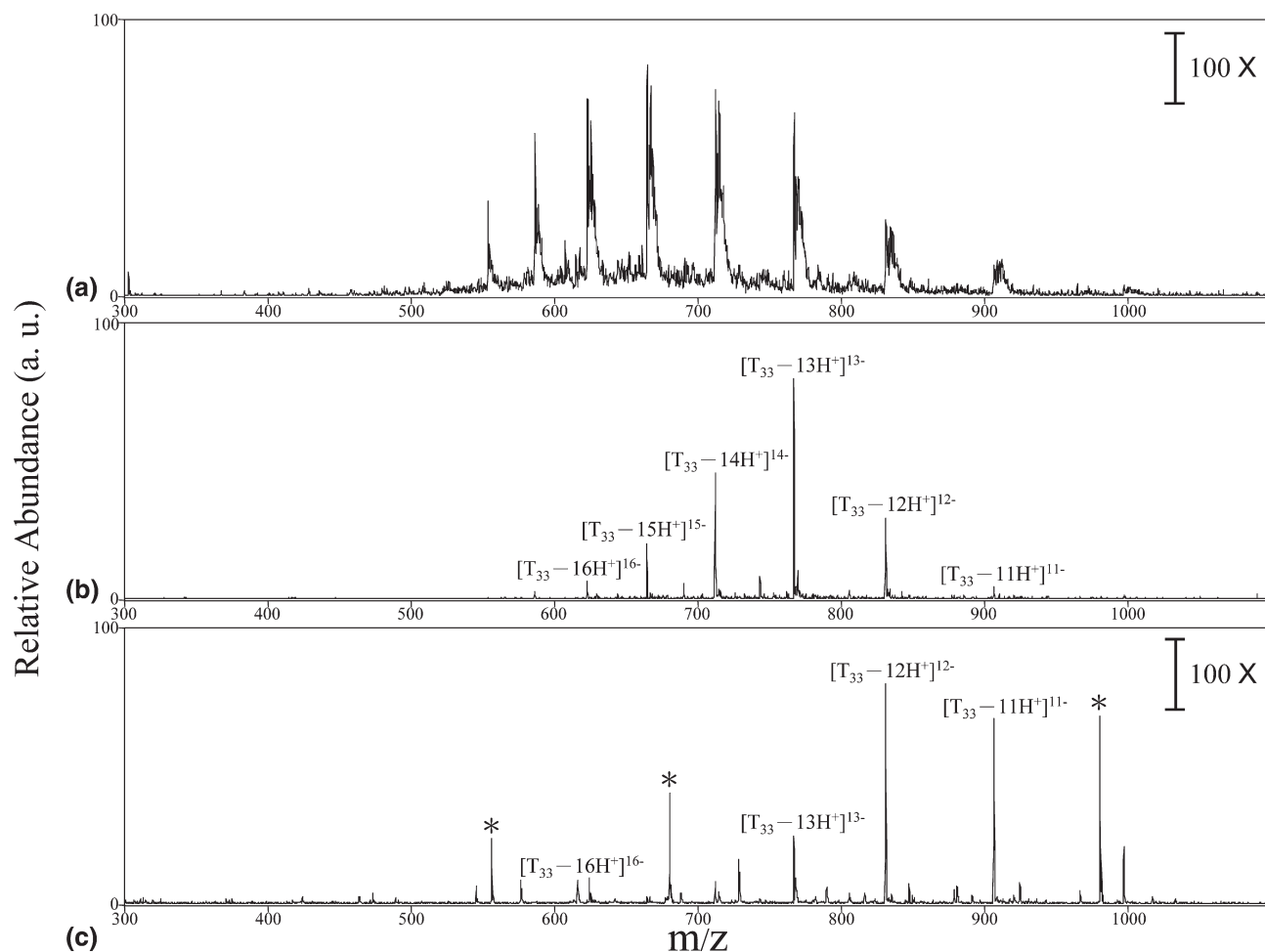
Figure 1. ESI-MS spectra of (**a**) T$_{33}$ (5 μM) in a solution containing 20% MeOH and (**b**), (**c**) T$_{33}$ (5 μM) in solutions containing 20% MeOH and (**b**) 5 mM and (**c**) 50 mM NH$_4$OAc (pH 7.0). The mass spectral intensities are plotted in arbitrary units (a.u.). The asterisks at m/z 556.1, 680.1, and 980.0 denote blank peaks that are also present in the spectrum of 50 mM NH$_4$OAc containing 20% MeOH.

50.0 μM Hg^{2+} ions, we obtained the maximum number of five Hg^{2+} ions bound onto T$_{33}$, i.e., the [T$_{33}$ + 5 Hg^{2+} − 23H$^+$]$^{13-}$ ion (Figure 2d). The mass resolution and peak intensity both decreased when the concentration of Hg^{2+} ions was greater than 50.0 μM.

Interaction Between T$_{33}$ and Other Metal Ions

Electrostatic interactions between the DNA phosphate backbone and metal ions can alter the conformation and ionization efficiency of DNA [19]. We conducted ESI-MS measurements to investigate the interactions between T$_{33}$ and various other metal ions, including Pb^{2+}, Ag$^+$, Fe^{3+}, Cr^{3+}, Ni^{2+}, Cu^{2+}, Co^{2+}, Zn^{2+}, and Cd^{2+}, at concentrations ranging from 5 to 50 μM. Figure 3 reveals that the fraction of T$_{33}$ toward Hg^{2+} ions is higher than those of the other metal ions. In a previous study using fluorescence spectroscopy, we found that the fluorescence intensity of the TOTO-3 · T$_{33}$ complex was enhanced 265-fold for Hg^{2+} over those of the other metal ions [6]. We note that different buffers (Tris-HCl and NH$_4$OAc/MeOH) and phases (liquid and gas) were

used in the two cases, leading to different selectivity values.

Effects of polyT Lengths in the Presence of Various Hg^{2+} or EthBr Concentrations

We investigated the impact of the length of the polyT on the interactions of DNA with Hg^{2+} ions and with EthBr molecules by using T$_7$, T$_{15}$, and T$_{50}$ as additional DNA strands, respectively. To maintain the same number of T bases as that of T$_{33}$ (5 μM), we set the concentrations of T$_7$, T$_{15}$, and T$_{50}$, at 23.5, 11, and 3.3 μM, respectively. As expected, the interactions of DNA with Hg^{2+} increased upon increasing the length of the polyT strand (Fig. S1, which can be found in the electronic version of this article). Similar to the behavior of T$_{33}$, the binding of the other three polyTs all exhibited a dependence on the Hg^{2+} concentration. Of the four tested polyTs, the interactions of T$_7$ with Hg^{2+} ions were the weakest, mainly due to its difficulty of forming a hairpin-like structure and its lower number of T units [6]. Figure S2
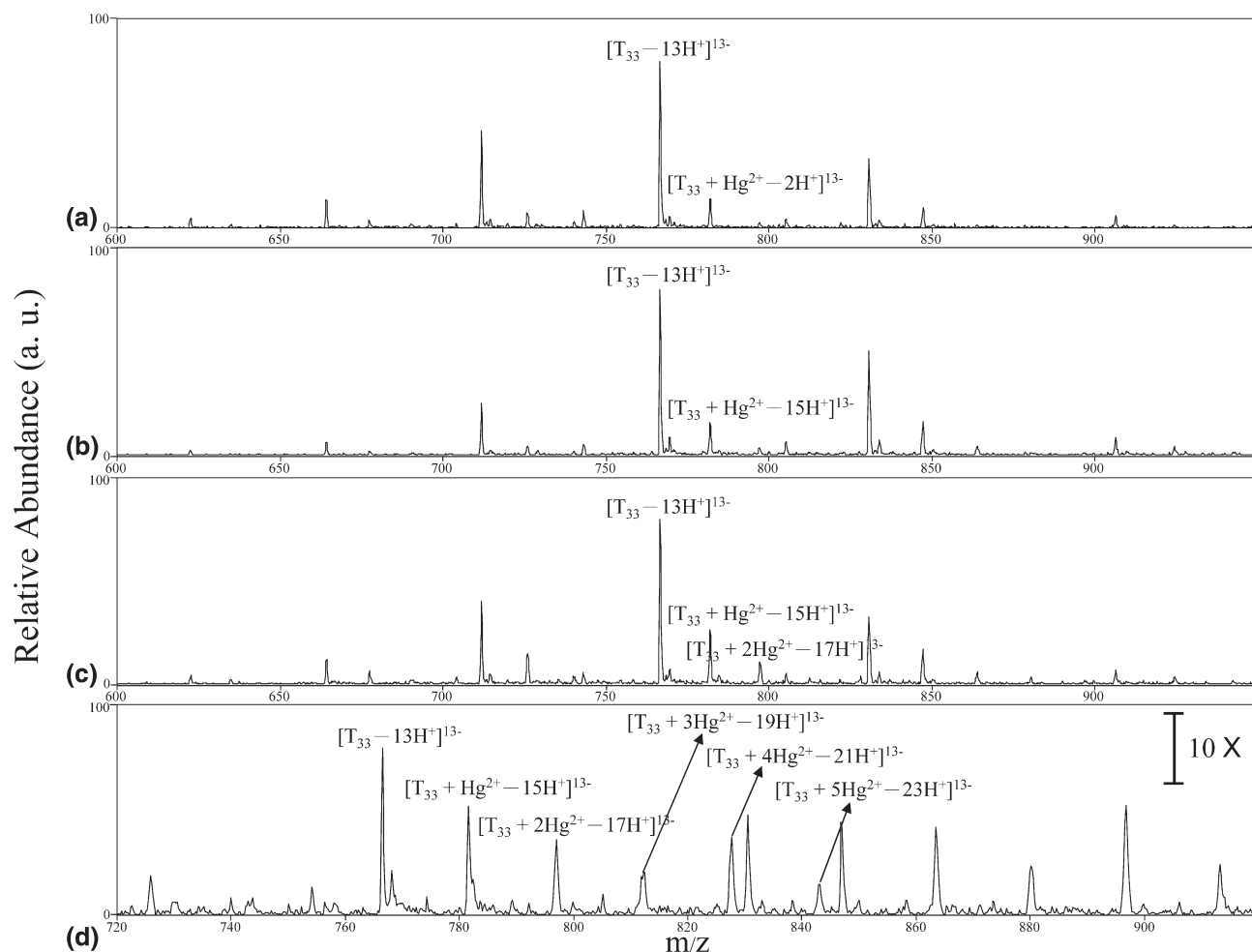
Figure 2. ESI-MS spectra of solutions containing T_{33} (5 μM), 20% MeOH, 5 mM NH_4OAc, and Hg^{2+} ions at concentrations of (**a**) 1, (**b**) 5, (**c**) 10, and (**d**) 50 μM. Other conditions were the same as those described in Figure 1.

reveals that the strengths of the interactions of the four polyT strands with EthBr increased upon increasing EthBr concentration (0–20 μM); the interaction strengths decreased in the order $T_{50} > T_{33} > T_{15} > T_7$.

### Interactions Among PolyT Strands, Hg^{2+} Ions, and EthBr

In the solutions composed of polyTs, EtBr (5.0 μM), and various Hg^{2+} concentrations (0–20.0 μM), several complexes were formed, including $[T_{33} + n\text{Ethidium} - (13 + n)H^+]^{13-}$, $[T_{33} + mHg^{2+} - (13 + 2m)H^+]^{13-}$, and $[T_{33} + n\text{Ethidium} + mHg^{2+} - (13 + 2m + n) H^+]^{13-}$, where m and n are integral, respectively). Upon increasing the Hg^{2+} concentration, the fraction of the polyT–EthBr complexes decreased, whereas those for the polyT–Hg^{2+} complexes increased (Figure 4.) PolyT–EthBr–Hg^{2+} complexes having binding stoichiometries of 1:1:1 occurred for the T_{15}, T_{33}, and T_{50} systems at Hg^{2+} concentrations of 2.5 μM; for the T_7-containing system, however, the 1:1:1 complexes occurred only at 20.0 μM Hg^{2+}. At this concentration of Hg^{2+} ions, 1:1:2 polyT–

EthBr–Hg^{2+} complexes formed for the T_{33} and T_{50} systems. Figure S3 displays peaks at m/z 805.8 and 821.0 for the $[T_{33} + Hg^{2+} + \text{Ethidium} - 16H^+]^{13-}$ and $[T_{33} +$
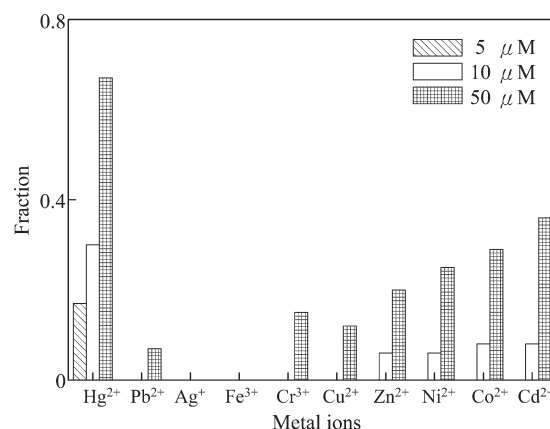
Figure 3. Fractions of T_{33}–metal ion complexes in solutions containing T_{33} (5 μM) and metal ions (5–50 μM). Other conditions were the same as those described in Figure 1.
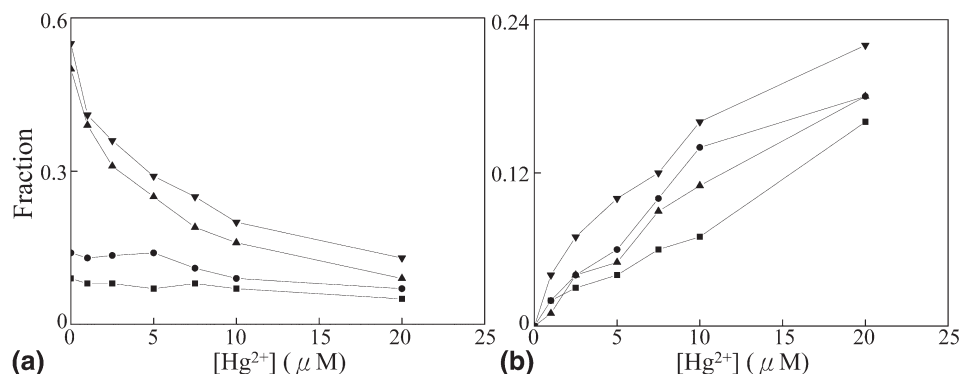
Figure 4. Fractions of (**a**) T_{33}–EthBr and (**b**) T_{33}–Hg^{2+} complexes in solutions containing polyT strands, EthBr (5 μM), and Hg^{2+} ions (0–20 μM), determined using ESI-MS. [filled square]: T_7 (23.5 μM); [filled circle]: T_{15} (11 μM); [filled triangle]: T_{33} (5 μM); [inverted filled triangle]: T_{50} (3.3 μM). Other conditions were the same as those described in Figure 1.

$2Hg^{2+} + Ethidium - 18H^+]^{13-}$, respectively, showing the existence of T_{33}–EthBr–Hg^{2+} complexes. These peaks signals increased upon increasing Hg^{2+} concentration (2.5–5.0 μM). Table 1 summarizes the effects of the Hg^{2+} and EthBr concentrations on the formation of the T_{33}–EthBr, T_{33}–Hg^{2+}, and T_{33}–EthBr–Hg^{2+} complexes. Greater concentrations of Hg^{2+} ions were required to form T_{33}–EthBr–Hg^{2+} complexes at higher EthBr concentrations. These results suggest that electrostatic interactions, but not intercalations, were the major forces between the EthBr molecules and the polyT strands. Upon increasing the concentration of Hg^{2+} ions in the polyT–EthBr–Hg^{2+} systems, the negative charge density of the DNA strands decreased, leading to their decreased interactions with EthBr.

Next, we examined the interactions of T_{33} with EthBr and Hg^{2+} ions in aqueous solution using fluorescence and CD spectroscopy. To minimize their consumption, we maintained the concentrations of both T_{33} and EthBr at 1.0 μM. Figure 5a displays the values of $(I_F - I_{F0})/I_{F0}$ for the T_{33}–EthBr and T_{33}–EthBr–Hg^{2+} complexes at Hg^{2+} concentrations ranging from 0 to 50.0 μM, where I_{F0} and I_F represent the fluorescence intensities of the T_{33}–EthBr and T_{33}–EthBr–Hg^{2+} complexes, respec-

tively. The fluorescence intensity of the solutions increased upon increasing the Hg^{2+} concentration in the range of 0–10.0 μM, while decreased in the range of 10.0–20.0 μM. At the low Hg^{2+} concentration, the fluorescence increase arose mainly from (1) the greater number of EthBr molecules intercalated with T_{33} as a result of the formation of a hairpin-like T_{33} structures, and (2) the increase in the quantum yield of the T_{33}–EthBr complexes when their structure became more rigid. In contrast, electrostatic repulsion disrupted the interactions between T_{33} and EthBr at high Hg^{2+} concentrations. Figure S4 displays that the fluorescence intensities of the solution composed of T_{33}, EthBr, and Hg^{2+} without/with conducting an annealing process were almost the same, showing that the temperature impact on the formation of the T_{33}–EthBr–Hg^{2+} complexes could be neglected. Figure 5b presents Job plots derived from solutions containing constant total concentrations of T_{33} and EthBr and various Hg^{2+} concentrations, suggesting that the T_{33}–EthBr complexes had approximate stoichiometries (T_{33}:EthBr) of 1:4, 1:2, and 2:1 at 1.0, 10.0, and 20.0 μM Hg^{2+}, respectively. These trends agree with our ESI-MS data (Table 1): upon increasing the Hg^{2+} ion concentrations, fewer EthBr

Table 1. Fractions of individual species in mixtures of T_{33}, EthBr, and Hg^{2+}, determined using ESI-MS[a]

Species	[Hg^{2+}] (μM)				
	0	1	5	10	20
[T_{33} + EthBr][b]	0.50 ($\pm$ 0.03)[d]	0.40 ($\pm$ 0.01)	0.25 ($\pm$ 0.01)	0.16 ($\pm$ 0.01)	0.09 ($\pm$ 0.007)
[T_{33} + Hg^{2+}][b]	N.D.[e]	0.01 ($\pm$ 0.001)	0.05 ($\pm$ 0.01)	0.11 ($\pm$ 0.01)	0.18 ($\pm$ 0.01)
[T_{33} + EthBr + Hg^{2+}][b]	N.D.	N.D.	0.06 ($\pm$ 0.01)	0.07 ($\pm$ 0.003)	0.07 ($\pm$ 0.004)
[T_{33} + EthBr + 2Hg^{2+}][b]	N.D.	N.D.	0.02 ($\pm$ 0.002)	0.02 ($\pm$ 0.001)	0.02 ($\pm$ 0.001)
[T_{33} + EthBr][c]	1.00 ($\pm$ 0.04)	0.87 ($\pm$ 0.03)	0.62 ($\pm$ 0.03)	0.40 ($\pm$ 0.03)	0.18 ($\pm$ 0.02)
[T_{33} + Hg^{2+}][c]	N.D.	N.D.	0.02 ($\pm$ 0.001)	0.03 ($\pm$ 0.002)	0.05 ($\pm$ 0.02)
[T_{33} + EthBr + Hg^{2+}][c]	N.D.	N.D.	N.D.	0.06 ($\pm$ 0.003)	0.06 ($\pm$ 0.004)
[T_{33} + EthBr + 2Hg^{2+}][c]	N.D.	N.D.	N.D.	0.02 ($\pm$ 0.001)	0.02 ($\pm$ 0.002)

[a]All T_{33} (5 μM) samples were prepared in solutions containing 5 mM NH$_4$OAc and 20% MeOH (vol/vol).
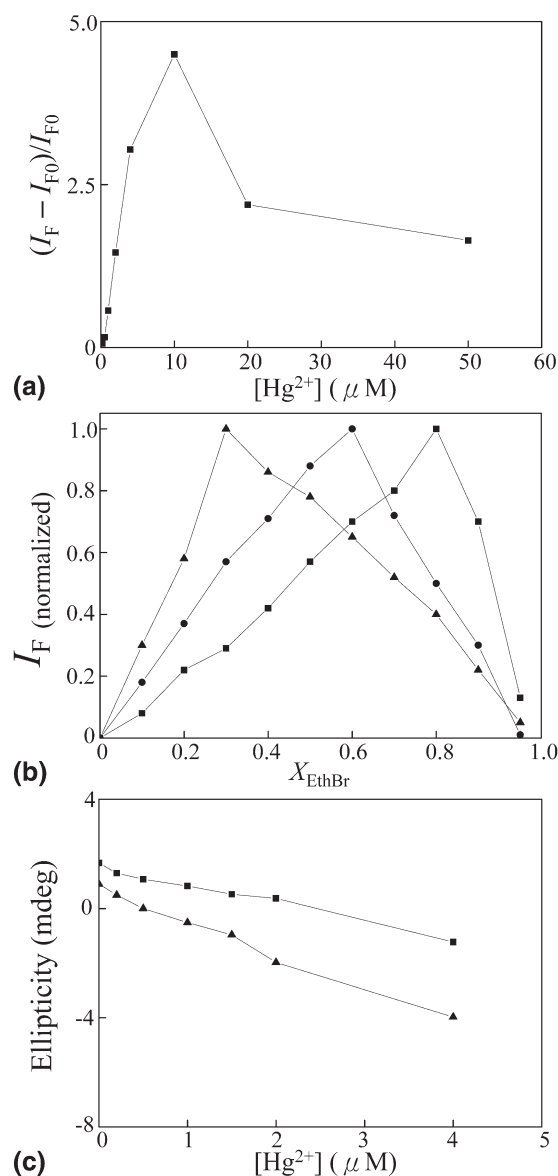[b][EthBr] = 5 μM.
[c][EthBr] = 10 μM.
[d]Value is in five replicate measurements.
[e]N.D. = not detected in the mass spectrum.

Figure 5. (**a**) Values of relative fluorescence $[(I_F - I_{F0})/I_{F0}]$ of solutions containing T_{33} (1 μM), EthBr (1 μM), and Hg^{2+} ions (0–50 μM). The samples were prepared in 5 mM NH$_4$OAc (pH 7.0) containing 20% MeOH; excitation wavelength: 530 nm. The fluorescence intensities (I_F) at 610 nm are plotted in arbitrary units (a.u.). (**b**) Job plot for EthBr binding to T_{33} ([EthBr] + [T_{33}] = 1 μM) in the presence of Hg^{2+} ([filled square]: 1 μM; [filled circle]: 5 μM; [filled triangle]: 20 μM). (**c**) Ellipticity at 280 nm of CD spectra for T_{33} (1 μM) in solutions containing 5 mM NH$_4$OAc and 20% MeOH and [filled square]) Hg^{2+} (0–4 μM) or [filled triangle] 1 μM EthBr and Hg^{2+} (0–4 μM). Other conditions were the same as those described in Figure 1.

molecules bonded to each T_{33} strand. We obtained similar results using CD spectroscopy (Figure 5c). The values of the ellipticity of the solutions containing T_{33} (1.0 μM) and EthBr (1.0 μM) at 280 nm decreased upon increasing the Hg^{2+} concentration from 0 to 4.0 μM, mainly as a result of the formation of a hairpin-like DNA structures.

Conclusions

We have used ESI-MS and fluorescence and CD spectroscopy to explore the interactions among polyT strands, EthBr, and Hg^{2+}. Those results reveal that the formation of T_{33}–EthBr–Hg^{2+} complexes is dependent on the concentrations of Hg^{2+} and EthBr. The results also reveal that Hg^{2+} ions have greater affinity toward polyT strands than do other metal ions. Our results provide useful information for developing DNA-based sensors for the detection of heavy metal ions. For instance, the sensitivity of DNA-conjugated gold nanoparticles for the detection of Hg^{2+} may be enhanced in the presence of intercalators that can further stabilize the DNA structures [28, 29]. Our approach also opens an avenue for studying the interactions of DNA with drugs in the presence and absence of metal ions, which may provide some potentially useful information for understanding drug activity and the role of metal ions on the biological function of DNA.

Appendix A
Supplementary Material

Supplementary material associated with this article may be found in the online version at doi:10.1016/j.jasms.2009.06.009.

References

1. Zahir, F.; Rizwi, S. J.; Haq, S. K.; Khan, R. H. Low Dose Mercury Toxicity and Human Health. *Environ. Toxicol. Pharmacol.* **2005,** *20,* 351–360.
2. Miyake, Y.; Togashi, H.; Tashiro, M.; Yamaguchi, H.; Oda, S.; Kudo, M.; Tanaka, Y.; Kondo, Y.; Sawa, R.; Fujimoto, T.; Machinami, T.; Ono, A. Mercury-Mediated Formation of Thymine–Hg–Thymine Base Pairs in DNA Duplexes. *J. Am. Chem. Soc.* **2006,** *128,* 2172–2173.
3. Ono, A.; Togashi, H. Highly Selective Oligonucleotide-Based Sensor for Mercury(II) in Aqueous Solutions. *Angew. Chem. Int. Ed. Engl.* **2004,** *43,* 4300–4302.
4. Xue, X.; Wang, F.; Liu, X. One-Step, Room Temperature, Colorimetric Detection of Mercury (Hg^{2+}) Using DNA/Nanoparticle Conjugates. *J. Am. Chem. Soc.* **2008,** *130,* 3244–3245.
5. Liu, C.-W.; Hsieh, Y.-T.; Huang, C.-C.; Lin, Z.-H.; Chang, H.-T. Detection of Mercury(II) Based on Hg^{2+}–DNA Complexes Inducing the Aggregation of Gold Nanoparticles. *Chem. Commun.* **2008,** 2242–2244.
6. Chiang, C.-K.; Huang, C.-C.; Liu, C.-W.; Chang, H.-T. Oligonucleotide-Based Fluorescence Probe for Sensitive and Selective Detection of Mercury(II) in Aqueous Solution. *Anal. Chem.* **2008,** *80,* 3716–3721.
7. Rosu, F.; Gabelica, V.; Houssier, C.; Colson, P.; De Pauw, E. Triplex and Quadruplex DNA Structures Studied by Electrospray Mass Spectrometry. *Rapid Commun. Mass Spectrom.* **2002,** *16,* 1729–1736.
8. David, W. M.; Brodbelt, J.; Kerwin, S. M.; Thomas, P. W. Investigation of Quadruplex Oligonucleotide-Drug Interactions by Electrospray Ionization Mass Spectrometry. *Anal. Chem.* **2002,** *74,* 2029–2033.
9. Rosu, F.; De Pauw, E.; Guittat, L.; Alberti, P.; Lacroix, L.; Mailliet, P.; Riou, J.-F.; Mergny, J.-L. Selective Interaction of Ethidium Derivatives with Quadruplexes: An Equilibrium Dialysis and Electrospray Ionization Mass Spectrometry Analysis. *Biochemistry* **2003,** *42,* 10361–10371.
10. Li, H.; Yuan, G.; Du, D. Investigation of Formation, Recognition, Stabilization, and Conversion of Dimeric G-quadruplexes of HIV-1 Integrase Inhibitors by Electrospray Ionization Mass Spectrometry. *J. Am. Soc. Mass Spectrom.* **2008,** *19,* 550–559.

11. Casagrande, V.; Alvino, A.; Bianco, A.; Ortaggi, G.; Franceschin, M. Study of Binding Affinity and Selectivity of Perylene and Coronene Derivatives Towards Duplex and Quadruplex DNA by ESI-MS. *J. Mass Spectrom.* **2009,** *44,* 530–540.

12. Pócsfalvi, G.; Landa, G. D.; Ferranti, P.; Ritieni, A.; Randazzo, G.; Malorni, A. Observation of Noncovalent Interactions Between Beauvericin and Oligonucleotides Using Electrospray Ionization Mass Spectrometry. *Rapid Commun. Mass Spectrom.* **1997,** *11,* 265–272.

13. Gabelica, V.; De Pauw, E.; Rosu, F. Interaction Between Antitumor Drugs and a Double-Stranded Oligonucleotide Studied by Electrospray Ionization Mass Spectrometry. *J. Mass Spectrom.* **1999,** *34,* 1328–1337.

14. Wan, K. X.; Shibue, T.; Gross, M. L. Noncovalent Complexes Between DNA-Binding Drugs and Double-Stranded Oligodeoxynucleotides: A Study by ESI Ion-Trap Mass Spectrometry. *J. Am. Chem. Soc.* **2000,** *122,* 300–307.

15. Rosu, F.; Gabelica, V.; Houssier, C.; De Pauw, E. Determination of Affinity, Stoichiometry, and Sequence Selectivity of Minor Groove Binder Complexes with Double-Stranded Oligodeoxynucleotides by Electrospray Ionization Mass Spectrometry. *Nucleic Acids Res.* **2002,** *30,* e82.

16. Mazzitelli, C. L.; Chu, Y.; Reczek, J. J.; Iverson, B. L.; Brodbelt, J. S. Screening of Threading Bis-Intercalators Binding to Duplex DNA by Electrospray Ionization Tandem Mass Spectrometry. *J. Am. Soc. Mass Spectrom.* **2007,** *18,* 311–321.

17. Mazzitelli, C. L.; Brodbelt, J. S.; Kern, J. T.; Rodriguez, M.; Kerwin, S. M. Evaluation of Binding of Perylene Diimide and Benzannulated Perylene Diimide Ligands to DNA by Electrospray Ionization Mass Spectrometry. *J. Am. Soc. Mass Spectrom.* **2006,** *17,* 593–604.

18. Duhamel, J.; Kanyo, J.; Dinter-Gottlieb, G.; Lu, P. Fluorescence Emission of Ethidium Bromide Intercalated in Defined DNA Duplexes: Evaluation of Hydrodynamics Components. *Biochemistry* **1996,** *35,* 16687–16697.

19. Wu, Q.; Cheng, X.; Hofstadler, S. A.; Smith, R. D. Specific Metal-Oligonucleotide Binding Studied by High Resolution Tandem Mass Spectrometry. *J. Mass Spectrom.* **1996,** *31,* 669–675.

20. Moon, S. T. M.; Schürch, S. Investigation of Metal–Oligonucleotide Complexes by Nanoelectrospray Tandem Mass Spectrometry in the Positive Mode. *J. Am. Soc. Mass Spectrom.* **2005,** *16,* 370–378.

21. Turner, K. B.; Monti, S. A.; Fabris, D. Like Polarity Ion/Ion Reactions Enable the Investigation of Specific Metal Interactions in Nucleic Acids and Their Noncovalent Assemblies. *J. Am. Chem. Soc.* **2008,** *130,* 13353–13363.

22. Mazzitelli, C. L.; Rodriguez, M.; Kerwin, S. M.; Brodbelt, J. S. Evaluation of Metal-Mediated DNA Binding of Benzoxazole Ligands by Electrospray Ionization Mass Spectrometry. *J. Am. Soc. Mass Spectrom.* **2008,** *19,* 209–218.

23. Reyzer, M. L.; Brodbelt, J. S.; Kerwin, S. M.; Kumar, D. Evaluation of Complexation of Metal-Mediated DNA-Binding Drugs to Oligonucleotides via Electrospray Ionization Mass Spectrometry. *Nucleic Acids Res.* **2001,** *29,* e103.

24. Tseng, W.-L.; Hsieh, M.-M.; Wang, S.-J.; Chang, H.-T. Effect of Ionic Strength, pH and Polymer Concentration on the Separation of DNA Fragments in the Presence of Electroosmotic Flow. *J. Chromatogr. A* **2000,** *894,* 219–230.

25. Tseng, W.-L.; Hsieh, M.-M.; Wang, S.-J.; Huang, C.-C.; Lin, Y.-C.; Chang, P.-L.; Chang, H.-T. Analysis of Large-Volume DNA Markers and Polymerase Chain Reaction Products by Capillary Electrophoresis in the Presence of Electroosmotic Flow. *J. Chromatogr. A* **2001,** *927,* 179–190.

26. Huang, M.-F.; Hsu, C.-E.; Tseng, W.-L.; Lin, Y.-C.; Chang, H.-T. Separation of dsDNA in the Presence of Electro-Osmotic Flow Under Discontinuous Conditions. *Electrophoresis.* **2001,** *22,* 2281–2290.

27. Rosu, F.; De Pauw, E.; Gabelica, V. Electrospray Mass Spectrometry to Study Drug–Nucleic Acids Interactions. *Biochimie* **2008,** *90,* 1074–1087.

28. Chen, S.-J.; Huang, Y.-F.; Huang, C.-C.; Lee, K. H.; Lin, Z.-H.; Chang, H.-T. Colorimetric Determination of Urinary Adenosine Using Aptamer-Modified Gold Nanoparticles. *Biosens. Bioelectron.* **2008,** *23,* 1749–1753.

29. Liu, C.-W.; Lin, Y.-W.; Huang, C.-C.; Chang, H.-T. Fluorescence Detection of Single-Nucleotide Polymorphisms using a Thymidine-Based Molecular Beacon. *Biosens. Bioelectron.* **2009,** *24,* 2541–2546.